Acta Crystallographica Section B
Structural Science
ISSN 0108-7681

Influence of fluoro-substitution on the planarity of 4-chlorobiphenyl (PCB 3)

G. Luthe,[a,b,c]* D. C. Swenson[d] and L. W. Robertson[a]

[a]Department of Occupational and Environmental Health, University of Iowa, 100 Oakdale Campus # 124 IREH, Iowa City, IA 52242-5000, USA, [b]University of Bremen, Institute for Inorganic and Physical Chemistry, Leobener Strasse, NW2, C2350, D-28334 Bremen, Germany, [c]Institute of Life Science and Technology, Saxion University of Applied Sciences, Enschede, The Netherlands, and [d]Department of Chemistry, University of Iowa, Iowa City, IA, USA

Correspondence e-mail: gregor-luthe@uiowa.edu

Received 19 September 2006
Accepted 13 December 2006

Accurate structure determinations by X-ray crystal analysis and computation using semi-empirical self-consistent field molecular orbital calculations are described and compared for five monofluorinated analogues of 4-chlorobiphenyl, *i.e.* 2-fluoro-4-chlorobiphenyl, 2′-fluoro-4-chlorobiphenyl, 3-fluoro-4-chlorobiphenyl, 3′-fluoro-4-chlorobiphenyl and 4′-fluoro-4-chlorobiphenyl. Intermolecular interactions for all monofluorinated isomers are dominated by phenyl–phenyl stacking and C—H–phenyl interactions. C—F bond lengths varied between 1.341 and 1.374 Å, C—Cl between 1.733 and 1.765 Å, and both correlate with electron-density differences as determined by ^{13}C NMR shifts. The interior ring angles at *ipso*-fluoro substitution increase up to 122.2–124.2° due to hyperconjugation by 2*p*-π-orbital overlapping, a phenomenon that was also reflected in the computer calculation. The angles of C—F and C—Cl relative to the aromatic ring for vicinal fluoro- and chloro substituents show an attraction, not a repulsion, between the adjacent F and Cl substituents. This finding is explained on the basis of electron donor and acceptor properties. The dihedral angles of *ortho*-substituted biphenyls show that monofluoro substitution results in slightly smaller increases compared with chlorine, while additional *ortho*-fluorination results in little further change in the dihedral angle. In contrast, *ortho*-chlorination strongly decreases the co-planarity. This is likely to be due to interior ring-angle distortion and the size of the halogen substituent. Fluoro substitution does indeed affect the planarity of the PCB3 analogues, but these effects are minor compared with chloro substitution. Fluorine tagging offers promise for use in *in vitro* and *in vivo* studies. Differences in computational *versus* measured data emphasize the need to use a variety of methods to ascertain the true nature of the physical properties of a compound.

1. Introduction

Polychlorinated biphenyls (PCBs) are a class of 209 persistent and ubiquitous environmental contaminants that have been manufactured for a large number of technical applications, *e.g.* for use in transformers and capacitors (Robertson & Hansen, 2001). PCBs have entered the environment through both their use and disposal. Laboratory and epidemiologic studies have implicated PCBs in a range of adverse health effects (Robertson & Hansen, 2001), such as cancer, heart disease, developmental toxicity and neurotoxicity. The mechanisms by which PCBs cause these adverse health effects are only poorly understood, partly because environmental PCBs are complex mixtures containing many PCBs. Many open questions remain.

Table 1
Receptor/enzyme interactions for PCBs.

Please note that direct binding of the PCBs themselves may not have been demonstrated, but is inferred by effect. Also note that the levels of the receptors themselves are in many cases influenced by PCB treatment. Much more work needs to be done in these areas. A more complete list and discussion may be found in Ludewig *et al.* (2007).

Abbreviation	Receptor	Ligands	Gene or function affected	Response references
AhR	Aryl hydrocarbon	'Coplanar', *meta*, *para* PCBs	CYP 1A	>20–30 fold (Bandiera *et al.*, 1982)
CAR	Constitutive androstane	*Ortho, para* PCBs	CYP 2B	>20–30 fold (Denomme *et al.*, 1983)
PXR	Pregnane X	Multi-*ortho* PCBs, PCB 47 and 184	CYP 3A	5–10 fold (Schuetz *et al.*, 1998; Hurst & Waxman, 2005)
PPAR	Peroxisome proliferator	'Coplanar', *meta*, *para* PCBs	CYP 4A	Repression (Ariyoshi *et al.*, 1998)

The dihedral angle between the benzene rings of the biphenyls seems to be one especially important determinant for the structure and hence for the biological activity of the PCBs. This angle depends on the substitution of the PCB, especially in the *ortho* positions (2, 2′, 6 and 6′) and strongly influences the binding of PCBs to binding sites within the cells. According to our review of the literature, the experimental dihedral angles for non-*ortho*-Cl-substituted PCBs are 35–45° (McKinney & Singh, 1988), mono 47–51° (Lehmler *et al.*, 2001; Kania-Korwel *et al.*, 2004; van der Sluis *et al.*, 1990), di 58–68° (Vyas *et al.*, 2006; Singh *et al.*, 1986) and tetra 86–87° (Singh & McKinney, 1979; Pedersen, 1975).

On the basis of what is now understood about the biochemical toxicology of PCBs, it appears that the dihedral angle directly influences the avidity of binding of PCBs to cellular and nuclear receptors, themselves mediators of signaling and gene expression. Table 1 gives an overview of the interactions of PCB congeners in receptor-mediated events. Much of the literature indicates that PCBs with no or few *ortho* chlorines are more coplanar and bind more avidly to the aryl hydrocarbon (Ah) receptor (see Table 1), and display a spectrum of toxic effects reflective of this binding (Bandiera *et al.*, 1982). As higher *ortho*-chlorine substitution occurs, binding avidity for the Ah receptor diminishes, while the binding avidity for the constitutive androstane (CAR) and pregnane X (PXR) receptors increases. These structure–activity relationships clearly demonstrate the importance of three-dimensional structure on the biologic/toxic activity of PCBs and related compounds.

One approach to gaining information about the three-dimensional structure of PCBs is from the X-ray analysis of single crystals; another is to compute the bond lengths and angles. Unfortunately, relatively few crystal structures of PCBs have been reported or computed. Therefore, we have completed and are reporting the crystal structures of the five monofluorinated PCBs 3 (F-PCBs 3) isomers and comparing these data with semi-empirical self-consistent field molecular orbital (SCF-MO) calculations. Table 2 gives a complete overview of the experimental X-ray data and Table 3 compares the bond lengths and angles of these F-PCBs 3 presented in this work. There is considerable general interest in using organic fluorines to probe the mechanisms of biochemical reactions (Ojima *et al.*, 1996; Tsushima *et al.*, 1982), and the synthesis of organo-fluorine compounds for pharmaceutical and biochemical applications (Welch & Eswarakrishnan, 1991). The research described here is an investigation of the utilization of fluorine-tagged persistent organic pollutants (POPs) as new marker compounds for the determination of metabolic pathways. Preliminary work on monofluorinated polycyclic aromatic hydrocarbons (F-PAHs) as internal standards and marker compounds was very promising (Luthe *et al.*, 2002); so, recently we synthesized a series of monofluorinated polychlorinated biphenyls (F-PCBs; Luthe, 2003; Luthe *et al.*, 2007) and polybrominated dibenzo-ethers (F-PBDEs; Luthe *et al.*, 2006).

The physical and chemical properties of F-containing organic compounds are related to a number of distinctive characteristics of the fluorine atom, including its radius, which is much smaller than that of the homologue chlorine. The van der Waals radii of fluorine and hydrogen are comparable, especially if C—F secondary binding (hyperconjugation) is taken into account. It is our aim to explore the potential of F-PCBs to investigate metabolic pathways and effects *in vitro* and *in vivo*. To achieve this goal we need to verify that fluorine tagging does not markedly change the three-dimensional structure of the molecule. This is especially true for the dihedral angle between the benzene rings. A significant change in this conformational parameter would likely change the biological effects of the F-PCBs, in comparison with their non-fluorinated analoges.

Our hypothesis is that fluorine tagging does not change the three-dimensional structure of a given PCB in a crucial way. To test this hypothesis, we have studied the crystal structures of a series of the five possible monofluorinated isomers of 4-chlorobiphenyl (PCB 3). PCB 3 would seem to be the most sensitive model system to determine conformation changes by substituents in the *ortho* positions due to the absence of substituents in the *ortho* positions as well as the absence of a buttressing effect of chlorines vicinal to the *ortho* positions.

The present research on F-PCBs is part of ongoing research focused on the synthesis, analytical and toxicologic aspects of monofluorinated analogues of POPs, their metabolites and adducts.

2. Experimental

2.1. Synthesis, compounds and crystallization

The F-PCBs 2-fluoro-4-chlorobiphenyl (3-2F), 2′-fluoro-4-chlorobiphenyl (3-2′F), 3-fluoro-4-chlorobiphenyl (3-3F), 3′-

Table 2
Experimental details of F-PCBs 3 isomers.

	3-3F	3-2F	3-2′F	3-3′F	3-4′F
Crystal data					
Chemical formula	$C_{12}H_8ClF$	$C_{12}H_8ClF$	$C_{12}H_8ClF$	$C_{12}H_8ClF$	$C_{12}H_8ClF$
M_r	206.63	206.63	206.63	206.63	206.63
Cell setting, space group	Orthorhombic, *Pbca*	Monoclinic, *C*2/*c*	Monoclinic, *C*2/*c*	Monoclinic, $P2_1/n$	Monoclinic, $P2_1/n$
Temperature (K)	190 (2)	190 (2)	190 (2)	190 (2)	190 (2)
a, *b*, *c* (Å)	11.9836 (7), 7.3820 (12), 21.670 (2)	17.4184 (17), 5.8649 (6), 19.4400 (19)	17.9426 (18), 6.0863 (6), 18.3206 (18)	11.3527 (11), 3.9099 (4), 21.920 (2)	9.5500 (10), 13.1441 (13), 15.6777 (16)
β (°)	90.00	104.981 (5)	103.701 (5)	99.966 (5)	96.323 (5)
V (Å^3)	1917.0 (4)	1918.4 (3)	1943.8 (3)	958.30 (16)	1956.0 (3)
Z	8	8	8	4	8
D_x (Mg m^{-3})	1.432	1.431	1.412	1.432	1.403
Radiation type	Mo $K\alpha$	Mo $K\alpha$	Mo $K\alpha$	Mo $K\alpha$	Mo $K\alpha$
μ (mm^{-1})	0.36	0.36	0.36	0.36	0.36
Crystal form, color	Needle, colorless	Prism, colorless	Prism, colorless	Prism, colorless	Prism, colorless
Crystal size (mm)	0.35 × 0.08 × 0.07	0.38 × 0.36 × 0.30	0.44 × 0.38 × 0.30	0.40 × 0.12 × 0.12	0.39 × 0.24 × 0.14
Data collection					
Diffractometer	Nonius KappaCCD	Nonius KappaCCD	Nonius KappaCCD	Nonius KappaCCD	Nonius KappaCCD
Data collection method	CCD φ and ω scans	CCD φ and ω scans	CCD φ and ω scans	CCD φ and ω scans	CCD φ and ω scans
Absorption correction	Multi-scan (based on symmetry-related measurements)	Multi-scan (based on symmetry-related measurements)	Multi-scan (based on symmetry-related measurements)	Multi-scan (based on symmetry-related measurements)	Multi-scan (based on symmetry-related measurements)
T_{min}	0.883	0.874	0.858	0.868	0.873
T_{max}	0.975	0.899	0.900	0.958	0.952
No. of measured, independent and observed reflections	34 729, 1691, 1367	18 886, 2192, 1952	32 179, 2217, 1708	14 766, 1679, 1430	32 179, 3447, 2412
Criterion for observed reflections	$I > 2\sigma(I)$	$I > 2\sigma(I)$	$I > 2\sigma(I)$	$I > 2\sigma(I)$	$I > 2\sigma(I)$
R_{int}	0.050	0.020	0.030	0.032	0.038
θ_{max} (°)	25.0	27.5	27.5	25.0	25.0
Refinement					
Refinement on	F^2	F^2	F^2	F^2	F^2
$R[F^2 > 2\sigma(F^2)]$, $wR(F^2)$, S	0.049, 0.144, 1.06	0.030, 0.083, 1.07	0.034, 0.097, 1.04	0.038, 0.098, 1.09	0.041, 0.111, 1.06
No. of reflections	1691	2192	2217	1679	3447
No. of parameters	127	127	131	167	326
H-atom treatment	Constrained to parent site	Constrained to parent site	Constrained to parent site	Constrained to parent site	Constrained to parent site
Weighting scheme	$w = 1/[\sigma^2(F_o^2) + (0.0686P)^2 + 2.4606P]$, where $P = (F_o^2 + 2F_c^2)/3$	$w = 1/[\sigma^2(F_o^2) + (0.0376P)^2 + 1.2786P]$, where $P = (F_o^2 + 2F_c^2)/3$	$w = 1/[\sigma^2(F_o^2) + (0.0509P)^2 + 0.6778P]$, where $P = (F_o^2 + 2F_c^2)/3$	$w = 1/[\sigma^2(F_o^2) + (0.0414P)^2 + 0.4269P]$, where $P = (F_o^2 + 2F_c^2)/3$	$w = 1/[\sigma^2(F_o^2) + (0.0529P)^2 + 0.3255P]$, where $P = (F_o^2 + 2F_c^2)/3$
$(\Delta/\sigma)_{max}$	< 0.0001	0.001	0.012	0.002	< 0.0001
$\Delta\rho_{max}$, $\Delta\rho_{min}$ (e Å^{-3})	0.31, −0.30	0.26, −0.25	0.20, −0.26	0.21, −0.25	0.17, −0.32

Computer programs used: *COLLECT* (Nonius BV, 1997–2000), *HKL Denzo*, *SCALEPACK* (Otwinowski & Minor, 1997), *SHELXTL*, Vol. 6.1 (Sheldrick, 2001).

fluoro-4-chlorobiphenyl (3-3′F) and 4′-fluoro-4-chlorobiphenyl (3-4′F) were synthesized by an improved method utilizing a palladium-catalyzed cross-coupling reaction, the so-called Suzuki-coupling (Luthe *et al.*, 2007). The coupling of chlorinated and/or fluorinated isomers of aryl boronic acids with bromo- and/or iodobenzenes afforded the desired F-PCB congeners in good to excellent yields. The first number refers to the corresponding PCB, the second indicates the position of the fluorine, with the chloro substituent having the highest priority. This Ballschmiter–Zell–Luthe (BZL) system (Luthe *et al.*, 2006, 2007) corresponds easily to the broadly used Ballschmiter–Zell (BZ) system (Ballschmiter & Zell, 1980) of the corresponding PCBs. All F-PCBs were re-crystallized from methanol. Their purity was determined to be >98% by GC-MS analysis.

2.2. X-ray structural determinations

Structure determinations of the five F-PCBs 3 isomers were routine. H atoms were located in difference maps but were constrained with the riding model [C—H = 0.95 Å, U_{iso}(H) = 1.2$U_{iso,eq}$(C)]. The 3-2′F, 3-3′F and 3-4′F isomers all exhibited disorder: ∼ 180° rotation of the C1′–C6′ phenyl ring about the C1—C1′ bond for the 3-2′F and 3-3′F isomers, an approximate inversion through the molecular centers for the 3-4′F isomer. (There are two independent molecules for the 3-4′F PCB

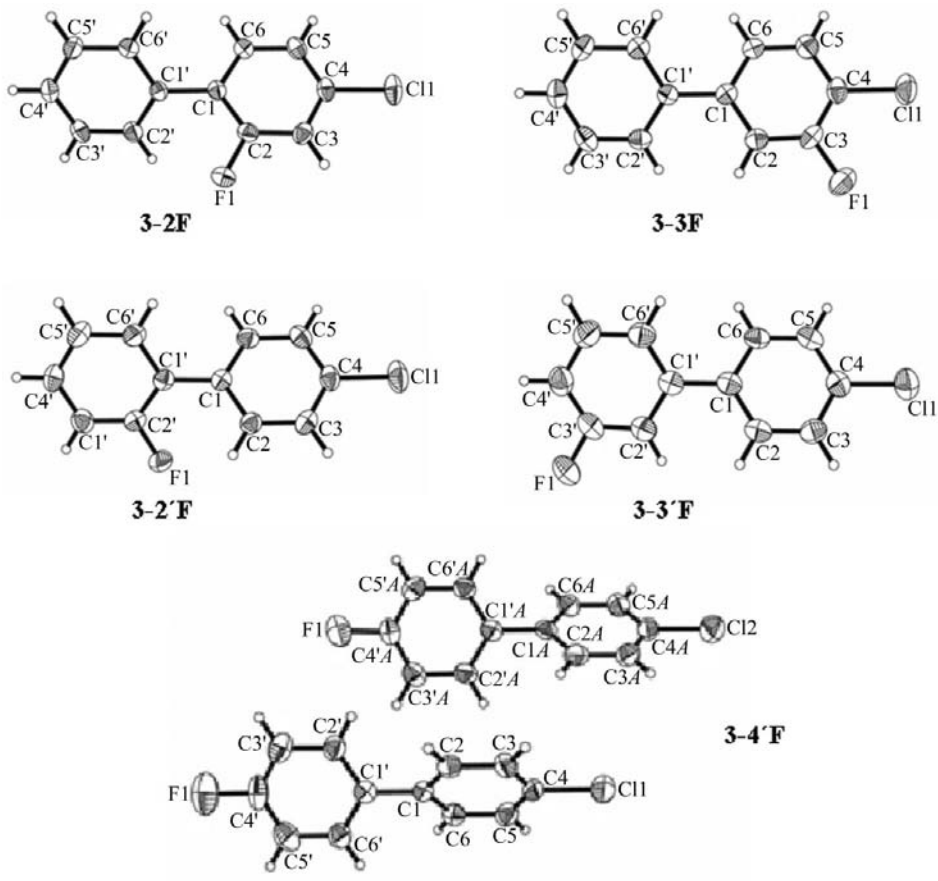

Figure 1
Ellipsoid plots (50% level) showing the F-PCBs 3: (*a*) 2-fluoro-4-chlorobiphenyl (3-2F), (*b*) 2′-fluoro-4-chlorobiphenyl (3-2′F), (*c*) 3-fluoro-4-chlorobiphenyl (3-3F), (*d*) 3′-fluoro-4-chlorobiphenyl (3-3′F) and (*e*) 4′-fluoro-4-chlorobiphenyl (3-4′F).

isomer.) Experimental details are given in Table 2. Details of the disorder refinement are included in the supplementary material.[1] Ellipsoid plots are shown in Fig. 1 and crystal packing in Fig. 2. Bond lengths and angles fall in the expected range with the exception of the C—F bonds in the 3-4′F isomers; s.u.s. are 0.0012–0.004 Å and 0.09–0.20°.

2.3. Database searches

Database searches were carried out on the November 2005 version of the Cambridge Structural Database (CSD; Allen, 2002); details are given in the supplementary material.

2.4. Molecular orbital computation with the SCF-MO method

The structures and conformations of the F-PCBs 3 were calculated using semi-empirical SCF-MO calculations with an Austin Model 1 (AM1) Hamiltonian (Dewar *et al.*, 1985). This was contained in the *Spartan´*02 package (http://www.wavefun.com/products/spartan.html) and carried out on a Quad 2.5 GHz Power Mac G5 with a PCI express graphic card. The heats of formation were computed using starting geometries similar to the optimized geometries. The use of symmetry constraints enhanced the convergence compared with completely unconstrained runs. Calculated values of the dihedral anlges are the average of the four torsion angles involving C1—C1′.

3. Results

3.1. C—F and C—Cl bond lengths and angles and dihedral angles

In general, the measured and computed bond lengths and angles of C—F and C—Cl are of similar magnitude, but do not necessarily follow the same trends, see Table 3. The phenyl rings for all F-PCBs 3 isomers are planar (r.m.s. deviations from planes range: 0.0010–0.008 Å). The measured dihedral angle between the least-squares of the phenyl rings shows the biphenyl twist angle, Ψ (C2—C1—C1′—C2′), as seen in Table 3. Ψ is *ca* 14° greater for the two *o*-F-substituted isomers [Ψ_{ave} = 50 (5)°] than for the other three isomers [Ψ_{ave} = 36 (5)°]. The differences within the isomers are minor for the computed twist angles ranging from 40.6 to 44.8° compared with the measured ones varying from 30.9 to 52.4°. However, in general the trends are comparable, *i.e.* 3-4′F shows the smallest twist angles, followed by 3-3F, 3-3′F, 3-2F and 3-2′F, see Table 3.

There is an interesting trend of increasing C–halogen bond length from the 3-2F isomer to the 3-4′F isomer (using the average C—Cl and C—F bond lengths for the 3-4′F isomer). This trend is not found by the compuational model. Although the difference between one isomer and the next in the series of increasing distance between halo substituents is (on average) < 3 s.u., the difference between the first and last in the series is > 7 s.u. for the C—Cl bond and > 10 s.u. for the C—F bond. Additionally, the effect of hyperconjugation between the phenyl ring and the F substituent is shown by the fact that the largest interior phenyl ring angle occurs at the site of F substitution for each isomer (range: 122.2–124.2°). This trend was also seen in the compuational data when comparing, for example, the C3′—C4′—C5′ angle in 3-4′F of 120.9° *versus* 119.3 to 119.8° for the other isomers; the C5′—C3′—C2′ angle in 3-3′F with 121.2° *versus* 119.5–120.1°; and the C3′—C2′—C1′ angle in 32′F with 121.8° *versus* 120.9–121.2°, see Table 3. There also appears to be an attractive intramolecular inter-

[1] Supplementary data for this paper are available from the IUCr electronic archives (Reference: BK5043). Services for accessing these data are described at the back of the journal.

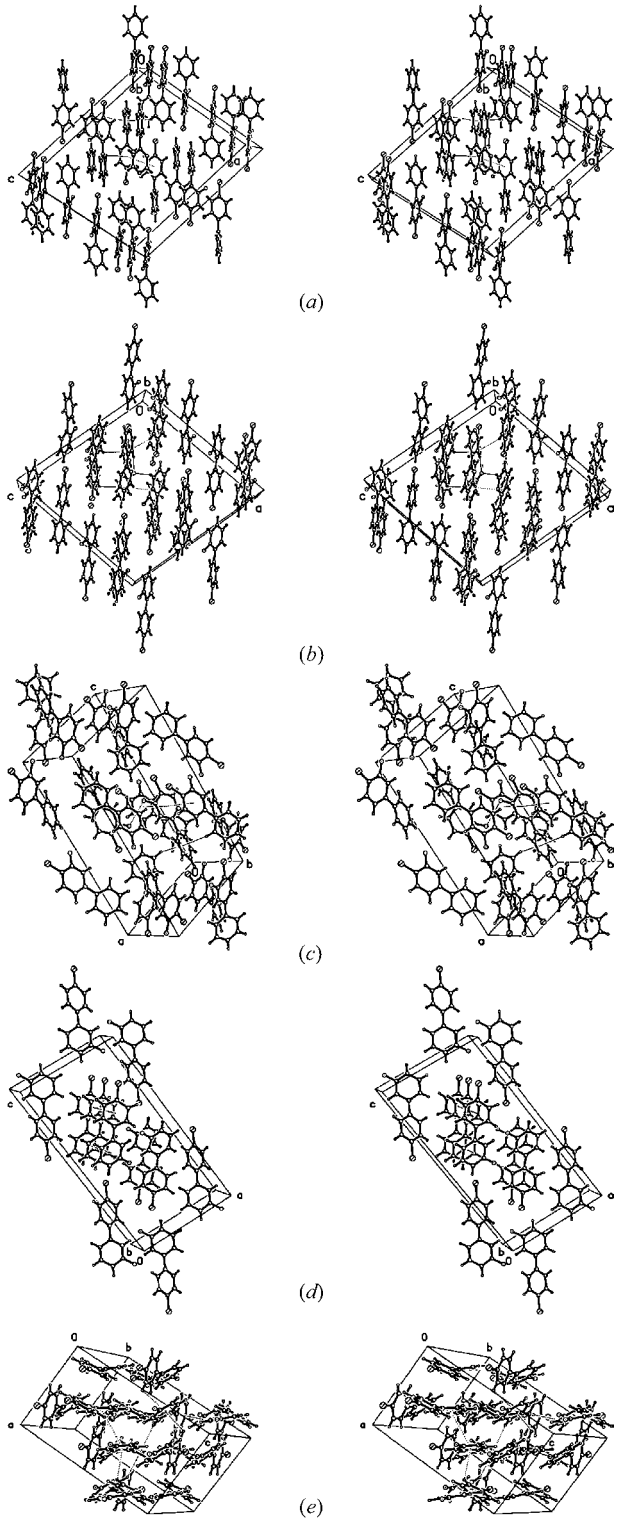

Figure 2
Stereo diagrams of the unit-cell contents showing intermolecular interactions (dotted lines). Atoms are shown as spheres of arbitrary size with the highest atomic number having the largest radius and the lowest the smallest. (*a*) 2-Fluoro-4-chlorobiphenyl (3-2F), (*b*) 2′-fluoro-4-chlorobiphenyl (3-2′F), (*c*) 3-fluoro-4-chlorobiphenyl (3-3F), (*d*) 3′-fluoro-4-chlorobiphenyl (3–3′F) and (*e*) 4′-fluoro-4-chlorobiphenyl (3-4′F).

action between the 3-F and 4-Cl substituents of the 3-3F isomer.

For the 3-4′F isomer the longer C—Cl bond and shorter C—F bond of molecule 1 correlate with the longer F···Cl molecular interaction between symmetry-related molecules 1. The shorter C—Cl bond and longer C—F bond of molecule 2 (labels with suffix *A*) correlate with the shorter F···Cl molecular interaction between symmetry-related molecules 2, see Tables 3 and 5, and Figs. 1 and 2.

A survey of Ψ values for simple 4-(mono)-substituted biphenyls found in the CSD show a range of 0–45° (see supplementary material). Three 4-Cl biphenyl structures with no *ortho* substitution were found in the CSD that show a Ψ range of 34–42°. Five 2-F(mono)-substituted biphenyls were found with a range of 48–53°, similar to the results reported here. Seven 2-Cl(mono)-substituted biphenyls were found with a range of 47–70°, one 2-Br(mono)-substituted biphenyl was found with Ψ = 61° and three 2-I(mono)-substituted biphenyls were found with a range of 75–85°. Additionally, six 2-Me(mono)-substituted biphenyl-like structures were found with a range of 42–66°. Table 4 lists the computed dihedral angels *versus* the measured ones. The values of the fluoro-substituted biphenyls are of comparable magnitude, while the chloro- and methyl-substituted isomers show larger angles in the computed model.

3.2. C—C bond lengths and angles

The C—C bond lengths and angles determined by X-ray and computed are in general in good agreement and of similar magnitude, see Table 3. A change by fluoro substitution in the C—C bond lengths and the interior angles in the biphenyl rings is observed by X-ray determination, but not seen in the computed data. The measurements show that the C1—C1′ bond is lengthened by fluoro substitution depending on the steric interaction, from 1.475 (3) Å for 3-4′F with no interaction to 1.489 (2) Å in 3-2F and 1.485 (2) Å in 3-2′F with *ortho* substitution. The computed C1—C1′ bond lengths are longer for the two *ortho*-substituted analogues 3-2F and 3-2′F both with 1.474 Å compared with 1.472 Å for the other isomers. The buttressing effects are apparently not taken into account in the computational model.

3.3. Packing of the F-PCBs 3 isomers

3.3.1. Crystal packing of 2-fluoro-4-chlorobiphenyl (3-2F). In 3-2F the molecules stack parallel to the *b* axis and the stacks are interconnected *via* $\pi\cdots\pi$, C—F···H—C and >C—F···H—C< interactions [Cg···Cg1^{i} 3.8114 (8) Å, Cg1···H2^{ii} = 3.039 Å, Cg···H5^{ii} = 3.019 Å, Cg2^{iii}···H5′ = 2.917 Å, F1···H6^{iv} = 2.536 Å; Cg1 = centroid of C1–C6, Cg2 = centroid of C1′–C6′; (i) $1-x, 1-y, 1-z$; (ii) $\frac{1}{2}-x, \frac{3}{2}-y, 1-z$; (iii) $\frac{3}{2}-x, \frac{3}{2}+y, \frac{3}{2}-z$; (iv) $x, 1+y, z$].

3.3.2. Crystal packing of 2′-fluoro-4-chlorobiphenyl (3-2′F). In 3–2′F the molecules stack parallel to the *b* axis and the stacks are interconnected *via* $\pi\cdots\pi$, C—H···π and >C—F···H—C< interactions [Cg1···H5^{i} = 3.287 Å, Cg1···H6^{ii} = 2.994 Å, Cg2···Cg2^{iii} = 3.790 (1) Å, Cg2···H3^{iv} = 3.051 Å,

Table 3
Bond lengths (Å), bond angles (°) and torsion angles (°) measured by X-ray compared with values computed by semi-empirical self-consitent field molecular orbital calculation (italics).

Structure	PCB 3 and F-PCBs 3						
specifications	3	3-2F	3-2′F	3-3F	3-3′F	3-4′F (1)	3-4′F (2)
Cl—C4		1.7381 (12)	1.7417 (14)	1.733 (3)	1.745 (2)	1.765 (2)	1.744 (3)
	1.740	*1.720*	*1.720*	*1.721*	*1.720*	*1.720*	*1.720*
F—C		1.3581 (13)	1.3613 (15)	1.341 (3)	1.374 (3)	1.360 (3)	1.395 (3)
	–	*1.342*	*1.343*	*1.342*	*1.340*	*1.339*	*1.339*
C1—C2		1.388 (2)	1.398 (2)	1.394 (4)	1.388 (3)	1.392 (3)	1.401 (3)
	1.406	*1.405*	*1.405*	*1.404*	*1.406*	*1.406*	*1.406*
C1—C6		1.399 (2)	1.392 (2)	1.400 (4)	1.403 (3)	1.398 (3)	1.392 (3)
	1.406	*1.407*	*1.407*	*1.407*	*1.406*	*1.406*	*1.406*
C1—C1′		1.489 (2)	1.485 (2)	1.488 (4)	1.485 (3)	1.479 (3)	1.475 (3)
	1.406	*1.474*	*1.474*	*1.472*	*1.472*	*1.472*	*1.472*
C2—C3		1.381 (2)	1.388(2)	1.373 (4)	1.385 (3)	1.382 (3)	1.377 (3)
	1.399	*1.394*	*1.399*	*1.394*	*1.399*	*1.399*	*1.399*
C3—C4		1.384 (4)	1.382 (2)	1.377 (4)	1.382 (3)	1.375 (3)	1.386 (4)
	1.392	*1.389*	*1.391*	*1.392*	*1.392*	*1.392*	*1.392*
C4—C5		1.380 (2)	1.379 (2)	1.375 (4)	1.380 (3)	1.372 (3)	1.374 (3)
	1.392	*1.393*	*1.392*	*1.393*	*1.392*	*1.392*	*1.392*
C5—C6		1.389 (2)	1.386 (2)	1.384 (4)	1.380 (3)	1.385 (3)	1.383 (3)
	1.399	*1.399*	*1.399*	*1.400*	*1.399*	*1.399*	*1.399*
C1′—C6′		1.396 (2)	1.401 (2)	1.404 (4)	1.397 (3)	1.395 (3)	1.403 (3)
	1.405	*1.405*	*1.407*	*1.405*	*1.407*	*1.407*	*1.407*
C1′—C2′		1.397 (2)	1.388 (2)	1.401 (4)	1.398 (3)	1.394 (3)	1.397 (3)
	1.405	*1.405*	*1.404*	*1.405*	*1.404*	*1.407*	*1.407*
C2′—C3′		1.389 (2)	1.375 (2)	1.386 (4)	1.379 (3)	1.383 (3)	1.381 (3)
	1.398	*1.398*	*1.395*	*1.398*	*1.392*	*1.397*	*1.397*
C3′—C4′		1.386 (2)	1.387 (2)	1.383 (4)	1.361 (4)	1.366 (4)	1.371 (3)
	1.392	*1.392*	*1.392*	*1.392*	*1.389*	*1.388*	*1.388*
C4′—C5′		1.390 (2)	1.383 (2)	1.383 (4)	1.388 (4)	1.378 (4)	1.374 (3)
	1.392	*1.392*	*1.393*	*1.392*	*1.392*	*1.388*	*1.388*
C5′—C6′		1.391 (2)	1.386 (2)	1.380 (4)	1.377 (3)	1.379 (3)	1.375 (3)
	1.398	*1.398*	*1.399*	*1.398*	*1.399*	*1.397*	*1.397*
C2—C1—C6		115.95 (10)	118.23 (12)	117.8 (2)	117.6 (2)	117.7 (2)	117.8 (2)
	118.1	*117.3*	*117.8*	*118.0*	*118.0*	*118.1*	*118.1*
C2—C1—C1′		122.92 (10)	121.59 (12)	121.6 (2)	121.8 (2)	121.6 (2)	121.5 (2)
	121.0	*121.9*	*121.2*	*121.0*	*121.0*	*121.0*	*121.0*
C6—C1—C1′		121.13 (10)	120.16 (11)	120.6 (2)	120.5 (2)	120.7 (2)	120.7 (2)
	121.0	*120.7*	*121.0*	*121.0*	*121.0*	*121.0*	*121.0*
C3—C2—C1		124.08 (11)	121.05 (13)	119.8 (3)	121.7 (2)	121.3 (2)	121.3 (2)
	121.1	*122.0*	*121.2*	*120.6*	*121.1*	*121.0*	*121.0*
C2—C3—C4		117.40 (11)	118.99 (13)	122.2 (3)	119.1 (2)	119.2 (2)	119.1 (2)
	119.8	*119.3*	*121.2*	*120.7*	*119.8*	*119.8*	*119.8*
C5—C4—C3		121.67 (10)	121.38 (12)	118.8 (3)	120.9 (2)	121.1 (2)	121.1 (2)
	120.3	*120.3*	*120.3*	*119.6*	*120.3*	*120.3*	*120.3*
C4—C5—C6		118.83 (11)	119.11 (13)	120.1 (3)	119.4 (2)	119.2 (2)	119.2 (2)
	119.8	*119.9*	*119.8*	*119.8*	*119.8*	*119.8*	*119.8*
C5—C6—C1		122.05 (11)	121.24 (13)	121.3 (3)	121.3 (2)	120.9 (2)	121.4 (2)
	121.1	*121.1*	*121.2*	*121.2*	*121.1*	*121.0*	*121.0*
C6′—C1′—C2′		118.85 (10)	115.68 (12)	118.1 (2)	117.9 (2)	117.86 (2)	117.5 (2)
	118.0	*117.7*	*117.3*	*117.9*	*118.0*	*118.2*	*118.2*
C6′—C1′—C1		120.41 (10)	121.37 (10)	120.1 (2)	121.6 (2)	120.8 (2)	121.4 (2)
	121.0	*121.2*	*120.8*	*121.0*	*121.0*	*120.9*	*120.9*
C2′—C1′—C1		120.70 (10)	122.94 (12)	120.1 (2)	120.6 (2)	121.1 (2)	121.2 (2)
	121.0	*121.0*	*121.9*	*121.0*	*121.0*	*120.9*	*120.9*
C3′—C2′—C1′		120.38 (11)	124.15 (13)	121.1 (3)	118.6 (2)	121.1 (2)	121.4 (2)
	121.1	*121.2*	*121.8*	*121.1*	*120.4*	*120.9*	*120.9*
C4′—C3′—C2′		120.35 (11)	118.55 (13)	120.0 (3)	124.2 (2)	118.2 (2)	118.2 (2)
	120.0	*120.1*	*119.9*	*120.1*	*121.2*	*119.5*	*119.5*
C3′—C4′—C5′		119.88 (11)	119.6 (13)	119.7 (3)	117.3 (2)	122.4 (2)	122.3 (2)
	119.8	*119.8*	*119.7*	*119.8*	*119.3*	*120.9*	*120.9*
C4′—C5′—C6′		119.87 (11)	120.35 (13)	120.4 (3)	120.5 (2)	118.4 (2)	118.5 (2)
	120.0	*120.1*	*120.2*	*120.1*	*119.9*	*119.5*	*119.5*
C5′—C6′—C1′		120.67 (11)	121.58 (13)	121.1 (3)	121.6 (2)	121.4 (2)	121.6 (2)
	121.1	*121.2*	*120.8*	*121.1*	*121.2*	*120.9*	*120.9*
F—C—C		F—C2—C1	F—C2′—C1′	F—C3—C2	F—C3′—C2′	F—C4′—C3′	F—C4′—C3′
	–	119.00 (10)	118.29 (11)	120.2 (3)	118.4 (2)	119.2 (2)	121.0 (2)
		117.7	*120.3*	*118.6*	*119.4*	*119.6*	*119.6*
F—C—C		F—C2—C3	F—C2′—C3′	F—C3—C4	F—C3′—C4′	F—C4′—C5′	F—C4′—C5′
	–	116.89 (10)	118.29 (11)	117.6 (2)	117.4 (2)	118.4 (2)	116.7 (2)

F1···H3^{v} = 2.550 Å, F1···H6 2.525 Å; Cg1 = centroid of C1–C6, Cg2 = C1′–C6′; (i) $\frac{1}{2}-x$, $\frac{1}{2}+y$, $\frac{1}{2}-z$; (ii) $\frac{1}{2}-x$, $\frac{1}{2}-y$, $1-z$; (iii) $1-x$, $1-y$, $1-z$; (iv) $\frac{1}{2}-x$, $\frac{3}{2}-y$, $1-z$; (v) $1-x$, $2-y$, $1-z$; (vi) $x, 1+y, z$]. Late refinement difference maps suggested a minor disorder of 180° rotation about the >C1—C1′< bond of the C1′–C6′ phenyl ring. The relative occupancy is refined to 0.9763 (15):0.0237 (15).

3.3.3. Crystal packing of 3-fluoro-4-chlorobiphenyl (3-3F). In 3-3F the molecules stack parallel to the *b* axis *via* $\pi\cdots\pi$ interactions [Cg···Cg^{i,ii} = 3.696 (2) Å; Cg1 = centroid of C1–C6; (i) $\frac{1}{2}-x, -\frac{1}{2}+y, z$; (ii) $\frac{1}{2}-x, \frac{1}{2}+y, z$]. The stacks of molecules are interconnected *via* C—H···π interactions [Cg2···H3′^{iii} = 2.776 Å, Cg···H6′^{ii} = 2.764 Å; Cg2 = centroid of C1′–C6′; (iii) $1-x$, $-\frac{1}{2}+y, \frac{1}{2}-z$] and F···F interactions [F···F^{iv} = 2.939 (3) Å; (iv) $1-x, 1-y, 1-z$].

3.3.4. Crystal packing of 3′-fluoro-4-chlorobiphenyl (3-3′F). In 3-3′F the molecules stack along the *b* axis *via* $\pi\cdots\pi$ interactions [Cg1···Cg1^{i,ii} = 3.910 Å, Cg2···Cg2^{i,ii} = 3.910 Å, Cg1 = centroid of C1–C6, Cg2 = centroid of C1′–C6′; (i) $x, -1+y, z$; (ii) $x, 1+y, z$]. The stacks are interconnected *via* >C—F···H—C< interactions [F···H^{iii} = 2.356 Å; (iii) $1-x, -y, 1-z$] and general van der Waals interactions between the stacks. The molecule was disordered (180° rotation about the >C1—C1′< bond of the C1′–C6′ ring. Two partial-occupancy molecules [occupancies refined to 0.874 (3):0.126 (3)] were used to model the disorder and were restrained to have the same conformation.

3.3.5. Crystal packing of 4′-fluoro-4-chlorobiphenyl (3-4′F). In the crystal packing of

Table 3 (continued)

Structure	PCB 3 and F-PCBs 3						
specifications	3	3-2F	3-2′F	3-3F	3-3′F	3-4′F (1)	3-4′F (2)
		120.2	*117.9*	*120.7*	*119.4*	*119.6*	*119.6*
C3—C4—Cl		118.64 (9)	119.53 (11)	120.2 (2)	119.3 (2)	119.3 (2)	119.11 (2)
	119.8	*119.9*	*119.9*	*120.8*	*119.9*	*119.9*	*119.9*
C5—C4—Cl		119.69 (9)	119.09 (11)	120.2 (2)	119.55 (15)	119.3 (2)	119.7 (2)
	119.8	*119.9*	*119.9*	*119.5*	*119.9*	*119.9*	*119.9*
Ψ†		52.45 (4)	46.72 (9)	30.86 (8)	34.9 (2)	38.9 (3)	41.4 (3)
	40.6	*44.0*	*44.8*	*40.7*	*40.9*	*40.7*	*40.7*

† Experimental values are dihedral angles between least-squares planes.

Table 4
Dihedral angles Ψ (°) ranges of mono-, di-, tri- and tetra-substituted biphenyls by fluorine, chlorine and methyl in the *ortho* positions X_i (i = 1–4).

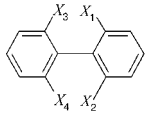

The dihedral angles are determined by averaging the four torsion angles involving the biphenyl (C1—C1′) bond of structures found in the Cambridge Structural Database and computed by semi-empirical self-consistent field molecular orbital calculation (italics). Note: values in parentheses are the number of structures found with the particular *ortho* substitution pattern.

	Dihedral angles Φ (°) of X_i-substituted biphenyls		
Substitution pattern	F (fluoro-)	Cl (chloro-)	CH_3 (methyl-)
None	0–0.45 (7)	0–0.45 (7)	0–0.45 (7)
	40.6	*40.6*	*40.6*
X_1	48–53 (5)	49–58 (7)	42–66 (6)
	50.4	*76.9*	*89.8*
X_1 X_2	41–58 (4)	81–84 (2)	67–87 (5)
	47.8	*90.0*	*90.0*
X_1 X_3	55–58 (2)	58–75 (4)	66 (1)
	58.8	*88.5*	*89.7*
X_1 X_2 X_3	–	83 (1)	–
	57.4	*89.9*	*90.0*
X_1 X_2 X_3 X_4	55–61 (10)	81–87 (2)	84–90 (4)
	65.8	*90.0*	*90.0*

3-4′F the two independent molecules of the 4′F isomer are aligned into columns parallel to the *b* axis *via* head-to-tail F···Cl interactions [F1—Cl1^{i} = 3.194 (5), F2—Cl2^{i} = 3.085 (3) Å; (i) $x, -1+y, z$]. Both molecules in the structure are disordered to the same extent. The second orientation for each molecule (labels with * and ″ suffix) can be approximated by inversion through the molecular center of mass. The conformation of the second orientation was restrained to be the same as the first orientation. The relative occupancies refined to 0.841 (3):0.159 (3). Molecule 2 (labels with '*A*' suffix) is approximately related to molecule 1 by $x+\frac{1}{2}, y+\frac{1}{4}, z$. $\pi\cdots\pi$ and C—H···π interactions connect columns of molecule 1 forming sheets approximately parallel with the $(10\bar{1})$ plane [Cg2···Cg2^{ii} = 3.987 (3), Cg2···H3^{iii} = 3.271 Å; Cg2 = centroid of C1′–C6′; (ii) $1-x, -y, 1-z$; (iii) $\frac{3}{2}-x, -\frac{1}{2}+y, \frac{3}{2}-z$]. C—H···$\pi$ interactions connect columns of molecule 2 forming sheets that fit between the sheets of molecule 1 [Cg4···H3A^{iv} = 3.195, Cg4···H5A^{v} = 3.089 Å; Cg4 = centroid of C1′A···C6′A; (iv) $\frac{1}{2}-x, -\frac{1}{2}+y, \frac{3}{2}-z$; (v) $-x, 1-y, 1-z$]. The sheets are interconnected by C—H···π interactions [Cg1···H2′A = 2.923, Cg1···H6′A^{vi} = 2.850, Cg3···H2′^{vii} = 2.808 Å; Cg1 = centroid of C1–C6, Cg3 = centroid of C1A–C6A; (vi) $1+x, y, z$; (vii) $\frac{1}{2}-x, \frac{1}{2}+y, \frac{3}{2}-z$] and C—H···F interactions (F2···H5′^{ii} = 2.682 Å).

4. Discussion

4.1. C—F and C—Cl bond lengths

The differences in C—F and C—Cl bond lengths may be explained on the basis of differences in electron density and orbital overlap. Many factors, *e.g.* mesomeric, *p*-inductive, steric and/or direct electric field effects, may alter the electron density. Substituent-induced chemical shifts in ^{13}C NMR reflect the actual distribution of electronic charges at the C atoms in the molecule. Therefore, instead of using semi-empirical SFC-MO calculations, we have relied on substituent-induced chemical shifts in ^{13}C NMR to determine the actual relative distribution of electron density, for the C positions 1–6, and 1′–6′. Higher shift values indicate a reduction in electron density, lower ones an increase. Both fluorine and chlorine substitution change the electronic factors and the substituents interact with each other. Since we are interested in the influence of fluorine, we investigated the electron distribution in biphenyl and 4-chlorobiphenyl (PCB3).

The following ^{13}C NMR shifts, δ (p.p.m.) in biphenyl were determined (Nishihara *et al.*, 2000): 141.18 (C1), 127.11 (C2, C6), 128.71 (C3, C5) and 127.20 (C4). For PCB 3 the following ^{13}C NMR shifts, δ (p.p.m.), were determined (Luthe *et al.*, 2006): 139.6 (C1), 128.4 (C2, C6), 129.0 (C3, C5), 133.3 (C4), 140.0 (C1′), 127.0 (C2′, C6′), 128.9 (C3′, C5′) and 127.6 (C4′). Comparing the shifts for C1′–C6′ in PCB 3 with C1–C6 in biphenyl demonstrates that the chlorine has a negligible effect on the non-substituted ring in PCB 3, with the exception of C1′ which has a higher shift ($\Delta\delta$ 1.18 p.p.m.). The C—F bond lengths [C2′—F 1.3613 (15), C3′—F 1.374 (3), C4′—F average 1.378 Å] are similar to 2-, 3- and 4-monofluoro-substituted biphenyls (C2—F: 1.348–1.364, C3—F: 1.356–1.367, C4—F: 1.356–1.390 Å; Oosaka & Akimoto, 1953). The two different C4′—F bond lengths are due to the effects of F···Cl intermolecular interactions in the crystal. The electron density decreases strongly ($\Delta\delta$ 1.4 p.p.m.) in the positions C2 and C6 relative to C2′ and C6′. The lower electron density in C2 relative to C2′ results in a shorter C2—F bond length [1.3581 (13) Å] compared with C2′—F [1.3613 (15) Å, although the difference is not statistically significant], since the carbon fluorine orbital overlap must be increased to gain the necessary electron density in the C—F bond. Comparing the positions C3 and C5 with C3′ and C5′, chlorine increases the

Table 5
Intermolecular interactions: phenyl···phenyl and phenyl···C—H (Å).

Isomer	Int. with Cg1	Int. with Cg1	Int. with Cg2	Int. with Cg2
3-2F	Cg1 3.811 (4)	H2′ 3.039	H5′ 2.917	H5 3.019
3-2′F	H5 3.286	H6′ 2.992	Cg2 3.790 (1)	H3 3.052
3-3F	Cg1 3.696 (2)	Cg1 3.696 (2)	H3′ 2.766	H6′ 2.764
3-3′F	Cg1 3.910 (2)	Cg1 3.910 (2)	Cg2 3.910 (2)	Cg2 3.91 (2)
3-4′F (1)	H2′*A* 2.923	H6′*A* 2.850	Cg2 3.987 (3)	H3 3.271
3-4′F (2)	H2′ 2.808		H3*A* 3.195	H5*A* 3.089

Note: Cg1 refers to the center of gravity of the C1–C6 phenyl ring and Cg2 refers to the center of gravity of the C1′–C6′ phenyl ring.

electron density only slightly ($\Delta\delta$ 0.1 p.p.m.) and is of minor influence.

C4—Cl bond lengths follow the same trend as the C—F bonds. The shortest C4—Cl bond (1.733 Å) is observed with an *ortho*-fluoro substituent and the longest with fluorine in the 4′ position (1.765 Å). This indicates that the C—F bond lengths result from the additive influences of fluoro and chloro substituents.

4.2. Influence of fluoro substitution on aromatic bond angles

X-ray analysis, microwave spectroscopy and SCF-MO computation show that the ring in fluorobenzene is distorted. This is caused by hyperconjugation of the 2*p* orbitals of the fluoro substituent with the aromatic π system. In chlorobenzene this effect is not observed, since the 3*p* orbitals of chlorine are too big to result in a good overlap. The fluoro-*ipso* bond angle C6—C1—C2 is widened to 123.4°, the C1—C2—C3 angle is narrowed to 118.0°, the remaining bond angles C2—C3—C4 and C3—C4—C5 are only slightly affected and show bond angles of 120.2°. The interior ring angles at *ipso*-fluoro substitution follow the same trend of distortion; values are between 122.2 (3) (3-3F) and 124.08 (11)° (3-2F).

Another observation was that the angles between aromatic vicinal fluoro and chloro substituents showed an attraction of the fluoro and chloro substituents. With the computational model we could not simulate this effect, since the C4—C3—Cl and C4—C5—Cl angles are identical with 119.9° in 3-3F, see Table 3. A closer look at the angles of chloro and fluoro substitution shows that these substituents are attracted to each other [F1···Cl1 = 2.887 (3) Å, C2—C3—F1 = 120.2 (3), C4—C3—F1 = 117.6 (2), C5—C4—Cl1 = 121.0 (2), C3—C4—Cl1 = 120.2 (2)°]. This appears on the surface to be very unusual, since one might expect that chloro and fluoro substituents should display repulsive behaviour towards each other. If the chlorine functions as an electron donor for the more electronegative electron acceptor fluorine, this would create a vicinal coupling through space. In addition, a hyper-conjugation might exist by the electron push-back from the 'hard' occupied fluoro-*p*-orbitals to the unoccupied chloro-*d*-orbitals. Both effects would tend to shorten the C3—F bond and C4—Cl bond. A search of the CSD for aromatic vicinal 1-Cl and 2-F substitutents (no 3 or 6 substitution) yields 17 such structures with the following results: C6—C1—C2 = 119.9 (6), C1—C2—C3 = 121.3 (7), C6—C1—Cl = 120.3 (4), C2—C1—Cl = 119.8 (6), C1—C2—F = 119.2 (5), C3—C2—F = 119.5 (9)°; C1—Cl = 1.727 (7), C2—F = 1.353 (7), C···F = 2.915 (17) Å.

4.3. Effect of fluorine on the dihedral angle

Comparing the dihedral angles in biphenyl affected by fluoro, chloro, methyl and no substituents in the *ortho*-positions (see Table 4), we observed that overall fluoro substitution has the smallest effect aside from hydrogen, followed by chloro and methyl substitution. A mono-fluoro substitution changes the dihedral angles to 48–53° (50.4° computed), with a mono-methyl substitution, 42–66° (89.8° computed), and a mono-chloro substitution, 49–70° (76.9° computed). The values for the chloro and fluoro substituents are surprisingly close to each other when comparing X-ray data, and similar to the value of no substitution, 0–45°.

This observation is due to the shorter bond length of the fluoro [1.341 (3)—1.374 (3) Å] compared with the chloro substituent [1.733 (3)–1.765 (2) Å]. Also, the distortion of the interior angle carrying the fluoro substituent [122.2 (3)–124.2 (3)°] reinforces the steric interaction. Both lead to a stronger interaction for a mono-fluoro substitution in the *ortho* positions (2, 2′, 6, 6′) than expected for the small size of fluorine (similar to hydrogen). The influence of the size difference of the substituent can be observed by comparing chloro with methyl substituents. Here the methyl group is more bulky and takes more space, and therefore increases the dihedral angle more strongly. Therefore, an increasing number of fluoro substituents in the *ortho* positions do not automatically lead to any further increase of the dihedral angles (X_1 = F: 48–53°, $X_{1,2}$ = F: 53–58, $X_{1,3}$ = F: 55–58° and $X_{1,2,3,4}$ = F: 55–57°), since their size is small. This is contrary to any other known substituent.

Values for chloro and methyl substituents are given in Table 4. The dihedral angles increase from 49 to 70° for mono-*ortho*-chloro substitution and from 81 to 87° for tetra-*ortho*-chloro substitution. A second (same ring) *ortho*-chloro substituent gives 81–84°. An *ortho*, *ortho*′ substitution leads to a smaller effect for chloro substitution (58–75°). This effect was not observed for fluoro substitution.

However, while the computed dihedral angles of fluoro-*ortho*-substituted biphenyls fit well with the measured data, the computed angles for the chloro- and methyl-substitued biphenyls do not fit well at all. The dihedral angles of the fluoro-*ortho* substitutions range between 50.4 (mono) and 65.7° (tetra), while the chloro and methyl substituted are between 76.9 (mono-chloro) and 90 (di-, tri- and tetrachloro), and 89.8 (mono-methyl) and 90° (di-, tri- and tetramethyl). This difference must be due to intermolecular interactions, since the semi-empirical SCF-MO calculations do not include these influences. The stacking reduces the dihedral angles of the chloro and methyl analogues, resulting in similar values to the fluoro-substitued analogues. This observation is very important for the interpretation of the biological acitivity of PCBs, since the dihedral angle is of major importance. The dihedral angle in a solvatization shell might differ strongly

from that determined by X-ray. Here SCF-MO calculations might be useful to compare these data. A similar conclusion was reached by Brock & Minton (1989) in their study of biphenyl fragments with no *ortho* substitution.

4.4. Influence of fluoro-tagging on the geometry of PCB 3

Investigation of geometry changes due to fluoro-tagging of PCB 3 by X-ray crystal analysis and SCF-MO calculations of the corresponding F-PCBs 3 shows that fluoro-tagging does indeed affect the geometry, *i.e.* the interior aromatic ring angles, the dihedral angle, C—Cl bond length and the packing of the crystals. However, these effects are much less than those found for chloro substituents and are not additive. Knowing the quality and magnitude of the resulting effects from fluoro-tagging of PCBs studied on PCB 3, we can justify the application of F-PCBs to analyze *in vitro* and *in vivo* metabolic pathways and effects. In fact, we will take advantage of these differences and will study the influence of the slight changes in the geometry on the biology, *e.g.* binding to cellular and nuclear receptors and their metabolism

4.5. Packing of the F-PCBs 3 isomers

The intermolecular interactions for all five isomers are dominated by $\pi\cdots\pi$ stacking and C—H$\cdots\pi$ phenyl interactions (see Table 5) and lead to crystal packings similar in nature to those found in the simple biphenyls that lack strong directional intermolecular forces such as hydrogen bonding. The 3-2F and 3-2′F isomers have very similar crystal packings. The 3-4′F isomer contains linear F$\cdots$Cl interactions: F1$\cdots$Cl1^{i} = 3.194 (5), F2*A* $\cdots$Cl2*A*^{i} = 3.085 (3) Å; (i) $x, 1+y, z$]. There is one other halo$\cdots$halo interaction in the 3-3F isomer: F1 $\cdots$F1^{ii} = 2.939 (3) Å [(ii) $1-x, 1-y, 1-z$]. Table 4 lists the metrics for the $\pi\cdots\pi$ and C—H$\cdots\pi$ interactions.

We would like to acknowledge Gerd-V. Röschenthaler, University Bremen, Germany, Udo A. Th. Brinkman and Freek Ariese, both of Free University, Amsterdam, The Netherlands, and Jan Scharp and Michiel van Buchem, both of Saxion University, Enschede, The Netherlands, for stimulating discussions. This work was financially supported by the Alexander von Humboldt Foundation, Bonn, Germany, and National Institute of Environmental Health Sciences grant P42 ES013661.

References

Allen, F. H. (2002). *Acta Cryst.* B**58**, 380–388.
Ariyoshi, N., Iwasaki, M., Kato, H., Tsusaki, S., Hamamura, M., Ichiki, T. & Oguri, K. (1998). *Environ. Toxicol. Pharmacol.* **5**, 219–225.
Ballschmiter, K. Z. & Zell, M. (1980). *Fresenius Z. Anal. Chem.* **302**, 20–31.
Bandiera, S., Safe, S. & Okey, A. B. (1982). *Chem. Biol. Interact.* **39**, 259–277.
Brock, C. P. & Minton, R. P. (1989). *J. Am. Chem. Soc.* **111**, 4586–4593.
Denomme, M. A., Bandiera, S., Lambert, I., Copp, L., Safe, L. & Safe, S. (1983). *Biochem. Pharmacol.* **32**, 2955–2963.
Dewar, M. J. S., Zoebisch, E. G., Healy, E. F. & Stewart, J. J. P. (1985). *J. Am. Chem. Soc.* **107**, 3902–3909.
Hurst, C. H. & Waxman, D. J. (2005). *Toxicol. Environ. Chem.* **87**, 299–311.
Kania-Korwel, I., Parkin, S., Robertson, L. W. & Lehmler, H.-J. (2004). *Acta Cryst.* E**60**, o1652–o1653.
Lehmler, H.-J., Parkin, S. & Robertson, L. W. (2001). *Acta Cryst.* E**57**, o111–o112.
Ludewig, G., Esch, H. & Robertson, L. W. (2007). *Handbuch der Lebensmitteltoxikologie*, edited by H. Dunkelberg, T. Gebel & A. Hartwig, ch. 20, pp. 1031–1094. Weinheim, Germany: Wiley-VCH.
Luthe, G. (2003). Kongenere chlorierte, bromierte und/oder iodierte fluorierte aromatische Verbindungen mit zwei Benzoringen in ihrer Grunsstruktur, Verfahren zu ihrer Herstellung und ihre Verwendung, German Patent, AZ 1020040075358.9, prioritiy date 24th July 2003.
Luthe, G., Ariese, F. & Brinkman, U. A. Th. (2002). *Handbook of Environmental Chemistry: Organic Fluorine Compounds*, edited by A. H. Neilson, pp. 249–275. Berlin, Germany: Springer Verlag.
Luthe, G., Leonards, P. E., Reijerink, G. S., Liu, H., Johansen, J. E. & Robertson, L. W. (2006). *Environ. Sci. Technol.* **40**, 3023–3029.
Luthe, G., Schut, B. G., Aaseng, J. E. & Johansen, J. E. (2007). *Chemosphere.* In the press.
McKinney, J. D. & Singh, P. (1988). *Acta Cryst.* C**44**, 558–562.
Nishihara, Y., Ikegashira, K., Toriyama, F., Mori, A. & Hiyama, T. (2000). *Bull. Chem. Soc. Jpn*, **73**, 985–990.
Nonius BV (1997–2000). *COLLECT*. Nonius BV, Delft, The Netherlands.
Ojima, I., McCarthy, J. R. & Welch, J. T. (1996). *Biochemical Frontiers of Fluorine Chemistry*. Am. Chem. Soc. Symp. Ser. 639. American Chemical Society, Washington DC, USA.
Oosaka, H. & Akimoto, Y. (1953). *Bull. Chem. Soc. Jpn*, **26**, 433–438.
Otwinowski, Z. & Minor, V. (1997). *Methods in Enzymology*, Vol. 26, *Macromolecular Crystallography* edited by C. W. Carter Jr & R. M. Sweet, Part A, pp. 307–326. New York: Academic Press.
Pedersen, B. F. (1975). *Acta Cryst.* B**31**, 2931–2933.
Robertson, L. W. & Hansen, L. G. (2001). *Recent Advances in the Environmental Toxicology and Health Effects of PCBs*. Lexington: University Press of Kentucky.
Schuetz, E. G., Brimer, C. & Schuetz, J. D. (1998). *Mol. Pharmacol.* **54**, 1113–1117.
Sheldrick, G. M. (2001). *SHELXTL*, Version 6.1. Bruker AXS Inc., Madison, Wisconsin, USA.
Singh, P. & McKinney, J. D. (1979). *Acta Cryst.* B**35**, 259–262.
Singh, P., Pedersen, L. G. & McKinney, J. D. (1986). *Acta Cryst.* C**42**, 1172–1175.
Sluis, P. van der, Moes, G. W. H., Behm, H., Smykalla, C., Beurskens, P. T. & Lenstra, A. T. H. (1990). *Acta Cryst.* C**46**, 2169–2171.
Tsushima, T., Kawada, K. & Tsuji, T. (1982). *Tetrahedron Lett.* **23**, 165–168.
Vyas, S. M., Parkin, S. & Lehmler, H. J. (2006). *Acta Cryst.* E**62**, o2905–o2906.
Welch, J. T. & Eswarakrishnan, S. (1991). *Fluorine in Bioorganic Chemistry*. New York: John Wiley.